Preventing Collapse Within Mass-Spring-Damper Models of Deformable Objects

ARTICLE · OCTOBER 1999

Source: CiteSeer

2 AUTHORS, INCLUDING:

Steve Maddock
The University of Sheffield
71 PUBLICATIONS **329** CITATIONS

Preventing Collapse Within Mass-Spring-Damper Models of Deformable Objects

Lee Cooper (L.Cooper@dcs.shef.ac.uk)
Steve Maddock (S.Maddock@dcs.shef.ac.uk)
Department of Computer Science
University of Sheffield
211 Portobello St., Sheffield, S1 4DP, UK.

Mass-spring-damper (MSD) models have been used by a number of researchers in attempts to model deformable objects. One of the main advantages of this approach is its simplicity. This means that it can be implemented quickly and it is also relatively easy to integrate with other techniques e.g. for collision detection or to impose constraints. However, the simplicity of the MSD models commonly used means that they can exhibit unwanted behaviour under certain conditions. The worst aspect of this is the tendency of MSD models to collapse under relatively small compressive forces. This paper presents a new robust model which prevents collapse.

1. Introduction

Computer models of deformable objects have a wide range of potential applications in a diverse range of fields including animation for entertainment [3] and medicine[12][14][6][7][4]. In order to create such models, several methods have been proposed. One approach [8][2][4][9][15][17] has been to use Finite Element and Finite Difference Methods [11] (FEM and FDM) which have been used for many years in engineering applications to model mechanical components and structures. These methods produce accurate results but are computationally expensive and complex. In order to create models which are fast to simulate and easy to extend, we have been concentrating on an alternative approach using MSD models [18][10][3][5]. Our aim is to use these to represent deformable human tissue in models of human limbs. This is a particularly demanding application since the model has to cope with the extreme deformation that occurs around joints. This paper describes a new model that has been developed for this purpose.

2. MSD Models

Figure 1 shows a typical two dimensional MSD model of a deformable ball resting on a fixed surface. The model consists of a number of point masses (the nodes) connected by springs and dampers (the edges). Although several arrangements of springs and dampers have been used, the most common one consists of a spring and damper connected in parallel as seen in figure 2. Here F is the force exerted by the damped spring at the endpoints, x is the current length of the spring, and k and l are the spring and damping constants respectively. The force exerted by this spring/damper arrangement is given by:

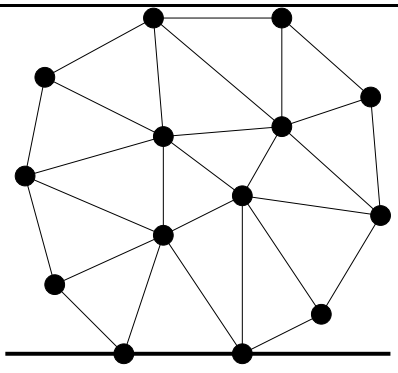

Figure 1: A 2D Mass-Spring-Damper mesh.

$$F = k(x_o - x) - l\dot{x} \tag{1}$$

where x_o is the original (rest) length of the spring.

In order to simulate an MSD mesh the resultant force acting on each point mass by the springs and dampers is computed. The acceleration of each point mass is then determined using Newton's second law. Then the velocity and position of the point masses are found using a suitable numerical integration technique (See [1] for more details).

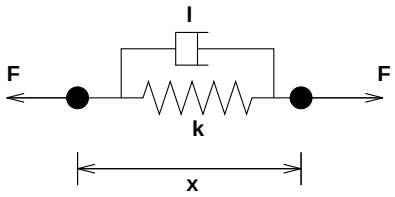

Figure 2: A damped spring.

3. Analysing Collapse in MSD Elements

In order to simplify this discussion we will deal with two dimensional meshes, although the ideas can be easily extended to three dimensions. We will also restrict the analysis to triangular meshes since meshes containing general polygons can be decomposed into triangular meshes. When modelling a deformable object using a triangular mesh each triangle can be thought of as an "element" of material. The behaviour of these basic elements (and the hence the model in general) can be altered by changing the way that the elements deform based on applied forces. In this paper, we will assume that the material being modelled is homogeneous and hence the behaviour of the elements throughout the material will be based on the same model even though their shape will vary.

Figure 3 shows a single element in a local coordinate system. Here the origin is made coincident with one of the vertices (A) and the x-axis is oriented such that it passes through a second vertex (B). The third vertex will then lie somewhere in the xy plane. In order to describe the current shape of a triangle, only three variables are required. In this case these are the x position of B and the x and y positions of C. If we consider the element shown in figure 3, then in general the element will exert a force on point C with the force vector $\underline{F}$ being a function of the following variables:

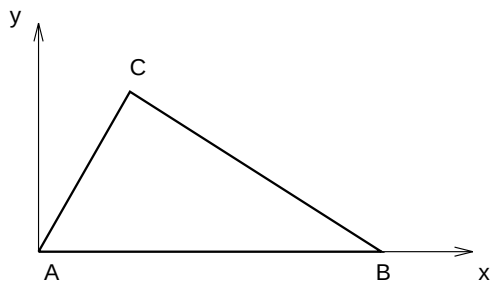

Figure 3: Triangular element in the local coordinate system.

$$\underline{F} = \underline{f}(\underline{B}, \underline{C}, AB_o, BC_o, CA_o, k) \tag{2}$$

where $\underline{B}$ and $\underline{C}$ are the position vectors of points B and C, AB_o is the initial length of edge AB (and similarly for the other edges), and k is a variable relating to the elasticity of the material. In its initial state, the element is assumed to be in its rest position where all the forces on the vertices are zero. As it stands, equation 2 is dependent only on the position of the points and not their velocities. Velocity information is needed to model damping forces within the element, however this will be ignored for now since we are primarily interested in the final equilibrium state of the elements after any transient motion has died down. The force function (2) determines the force that is exerted by the elements on the point masses and hence the behaviour of the material. In order to compute the forces on a particular point mass within the mesh due to a particular element, we transform the element into the local coordinate system such that the point we are calculating the force for lies in the xy plane (corresponding to C) and the other vertices for the element are in positions corresponding to A and B (i.e. at the origin and aligned with the x-axis).

This is illustrated in figure 4. This method of applying a local coordinate system allows the problem of element design to be reduced to the problem of designing a suitable force function.

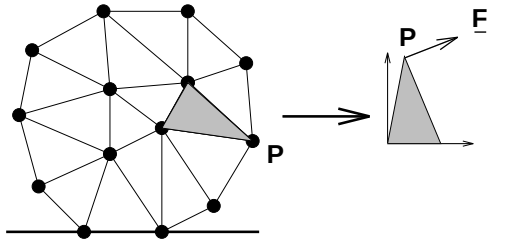

Figure 4: Computing the force exerted on a point mass by an element.

3.1 Standard Element

The simplest element design uses three linear springs along the edges of the element. This gives the following force function (note that damping forces are excluded):

$$\underline{F} = k(CA_o - |\underline{C}|)\frac{\underline{C}}{|\underline{C}|} + k(BC_o - |\underline{BC}|)\frac{\underline{BC}}{|\underline{BC}|} \quad (3)$$

where $\underline{BC} = \underline{C} - \underline{B}$ according to standard vector notation. In order to consider how the force on C changes as it moves with respect to A and B, the function was evaluated for the situation where $AB_o = 1$, $BC_o = 1$, $CA_o = \sqrt{2}$, $k = 1$, $\underline{B} = \binom{1}{0}$, and the point C is moved in the positive xy quadrant. These values of AB_o, BC_o and CA_o correspond to the rest state shown in figure 5.

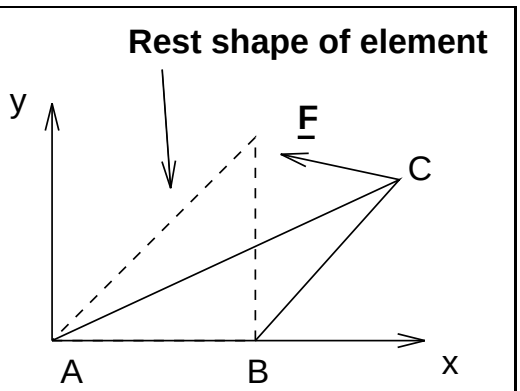

Figure 5: Force on C as it moves in the plane.

The magnitude of the force on C is shown on the graph in figure 6. The graph shows two points at which the force is zero. One is at the initial position of $\binom{1}{1}$ and the other occurs on the x axis around $\binom{0.6}{0}$. This second point occurs when the forces from the two springs (AC and BC) cancel each another out. The shape of this graph indicates why meshes composed of this type of element readily collapse. If we consider the element being compressed vertically, then we can see that if a suitably large force is applied it is possible to push C such that it lies on the x-axis. Consideration of the force function also shows that the graph below the x-axis (not shown) is a mirror image of that above. This means that there is a third point where the force acting on C becomes zero at $\underline{C} = \binom{1}{-1}$ (due to the spring lengths becoming equal to their rest length) as illustrated in figure 7.

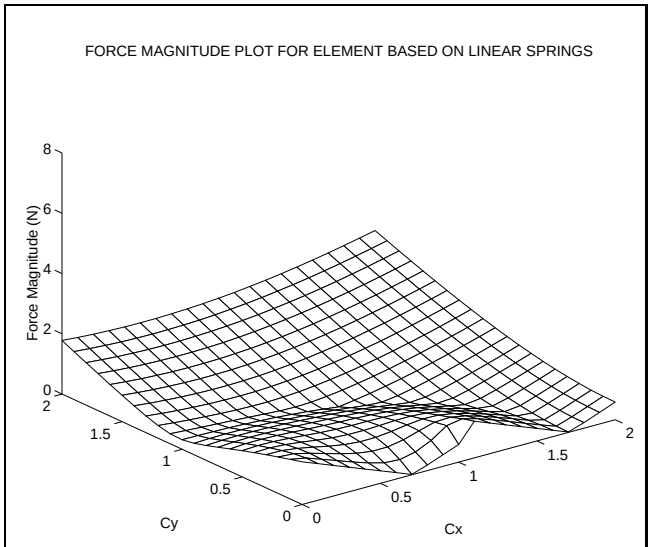

Figure 6: Magnitude of the force on C at different points within the plane.

This gives rise to two major problems. Firstly, it is possible to push the vertices past the opposite edge if a suitably large force is applied. In a realistic model this would not be possible since as the point approached the edge the material within the element would become more and more compressed producing reaction forces on C which tended to infinity as the point tended towards the edge. Secondly, the problem is compounded by the fact that if the point does cross the line through the opposite edge, then the element flips into an alternative state where the reaction forces act towards the rest point on the wrong side of the line. The term "flip" is appropriate since if these elements are simulated and this situation occurs the element suddenly changes shape. Another result of this "flipping" behaviour is the fact that even if the compression force is removed the element does not regain its original shape unless a stretching force is applied which is sufficient to flip the element back into the correct configuration. In order to try and prevent this collapse, we need to use a different force function. This is considered in the next section.

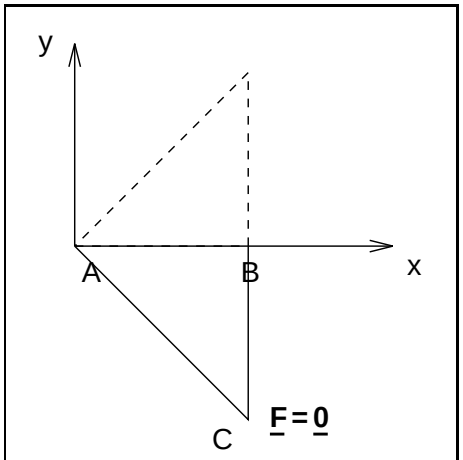

Figure 7: Alternative rest point.

4. Preventing Collapse

This section describes a number of methods that have been considered by ourselves and other researchers to try and prevent collapse occuring. It then describes a new method which we have developed.

4.1 Element Containing Springs to the Centroid

One approach that has been suggested [18] involves adding three more springs from the vertices to the centroid of the element. The reasoning behind this approach is that as the standard element is compressed its resistance to further compression reduces since the springs become less and less aligned with the crush direction. However, with springs to the centroid it is hoped that at least one of the springs should remain reasonably well aligned. The force magnitude plot for this element design is shown in figure 8. The graph shows that these extra springs make very little difference to the force function and the element will still compress fully if a suitably large force is applied. This is due to the fact that the linear springs used can be compressed fully. The next section considers the use of an alternative non-linear spring.

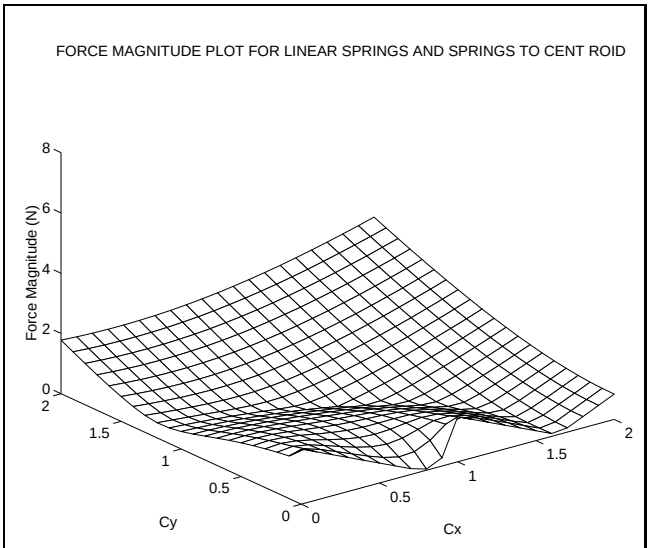

Figure 8: Force magnitude for springs along edges and to centroid.

4.2 Element Composed of Non-Linear Springs

In reality springs do not behave in a linear manner when highly compressed. Generally, as the spring length tends towards zero the spring will exert reaction forces which tend to infinity. In order to try and model this effect, we have devised the following function for a non-linear spring which resists collapse:

$$\begin{aligned} f &= k(x_o - x) + \frac{kx_o^2}{x} - kx_o \\ &= k(\frac{x_o^2}{x} - x) \end{aligned} \quad (4)$$

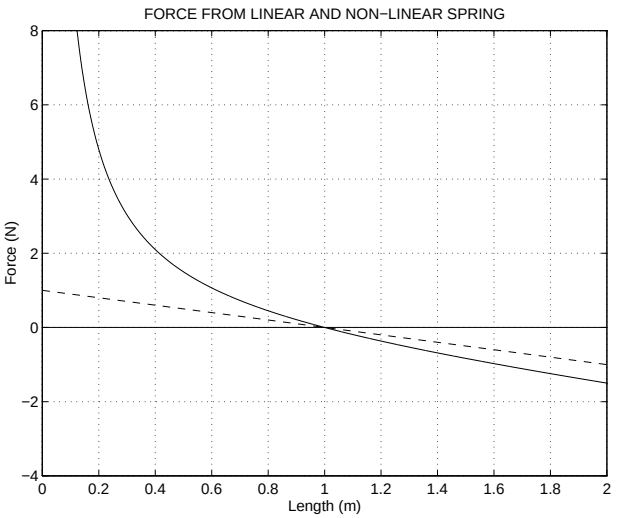

Figure 9: Linear spring (broken line); Non-linear spring (solid line).

This combines the term for a linear spring with a non-linear term which tends to infinity as x tends to 0. The $-kx_o$ is also needed to ensure that $f = 0$ at $x = x_o$. A graph of the force exerted by this spring as a function of the displacement is shown in figure 9 (for $k = 1$, $x_o = 1$), together with the force from a linear spring. If we now replace the linear springs in the standard element with the new non-linear spring, we obtain the force magnitude plot shown in figure 10.

It can be seen that the force required to crush the element such that C is close to points A and B now becomes very large (tending to infinity as C tends towards the points themselves). However, there are still points along the x axis at which the force is finite, indicating that it is still possible to flip the element.

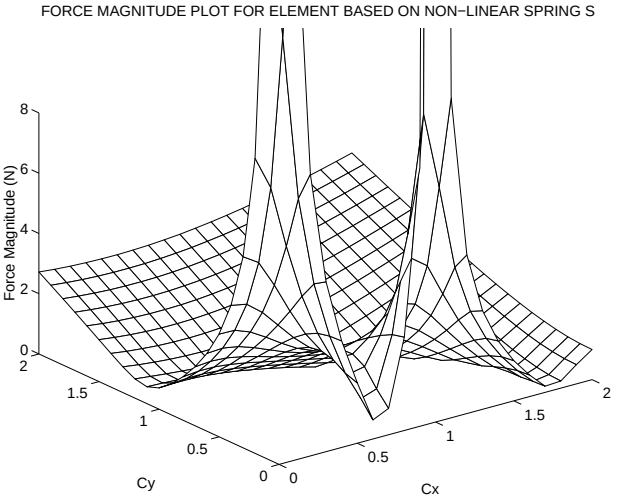

Figure 10: Element using non-linear springs.

4.3 A New Element Design Based on Edge Repulsion Forces

In order to prevent this, a new type of spring is presented which exerts a force based on the perpendicular distance of the point from the opposite edge. The force is always away from the edge and its magnitude is given by the non-linear spring function in equation 4.

This method can essentially be thought of as the edges exerting a repulsion force on the points opposite which act directly away from the edges. This is illustrated in figure 11. A new element has been designed which consists of three damped linear springs along the edges and edge repulsion springs for each point. This will be referred to as the "ER" (edge repulsion) element. The new force function is given by,

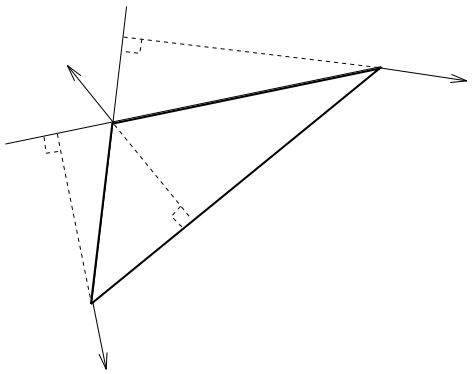

Figure 11: Edge repulsion forces.

$$\begin{aligned} \underline{F} &= k(CA_o - |\underline{C}|)\frac{\underline{C}}{|\underline{C}|} + k(BC_o - |\underline{BC}|)\frac{\underline{BC}}{|\underline{BC}|} \\ &+ k(\frac{EC_o^2}{|\underline{EC}|} - |\underline{EC}|)\frac{\underline{EC}}{|\underline{EC}|} \end{aligned} \quad (5)$$

where E is the projection of C onto the line passing through AB, and has a position vector given by $\underline{E} = \binom{C_x}{0}$.

The force magnitude graph for this new element is shown in figure 12. It can be seen that the reaction force now becomes infinite as we tend towards the x-axis, thus preventing the element from collapsing.

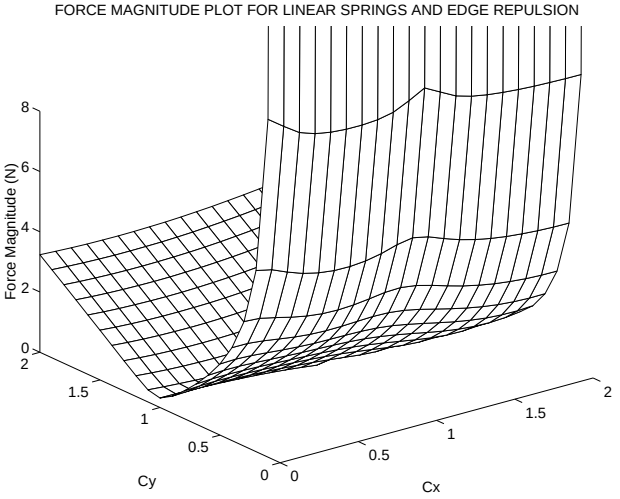

Figure 12: Magnitude of force on C for ER-element.

5. Results Using the New Model

This section describes a system that has been implemented to test the new element along with results that have been obtained. The simulation system uses a simple Euler method (see [13] for details) for computing the new position and velocity variables of the particles after each time step. We also implement a simple constraint method in which point masses can be attached to rigid bodies (represented by closed polygons in 2D). In order to test the new elements, a highly simplified model of a limb was used (see figures 13 and 14). This consists of two rigid bodies (bones) surrounded by a layer of deformable material (tissue). The upper bone is held in a fixed position whilst the lower one is rotated around a point between the two bodies (representing a simple hinge joint). The first series of images shows the deformation which occurs when the standard elements are used (damped linear springs along each edge).

Figure 13a shows the limb in the initial straight position. At this stage, all the elements are in their rest state. The joint angle was then slowly increased at a rate of approximately 10 degrees per second of simulation time. At 45 degrees (figure 13b) some of the elements are already showing considerable compression, particularly around the inside corner of the joint. At 47 degrees (figure 13c) one of the elements collapses. At this stage the motion of the limb was stopped and the collapsed element eventually settled at the shape shown

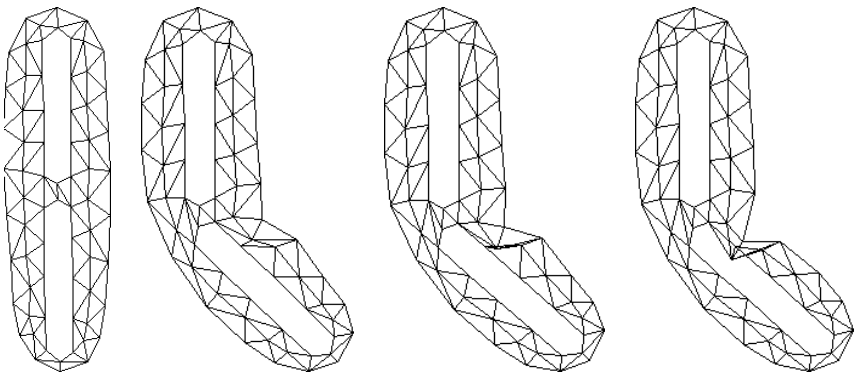

(a) Initial state.

(b) 45 degrees - just before collapse.

(c) 47 degrees - onset of collapse.

(d) 47 degrees - after collapse.

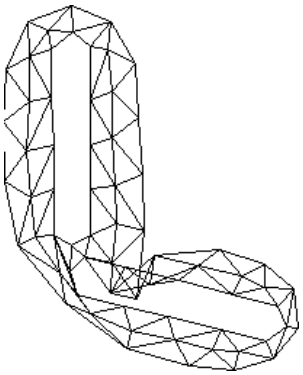

(e) 75 degrees.

Figure 13: Deformation of standard elements at different joint angles.

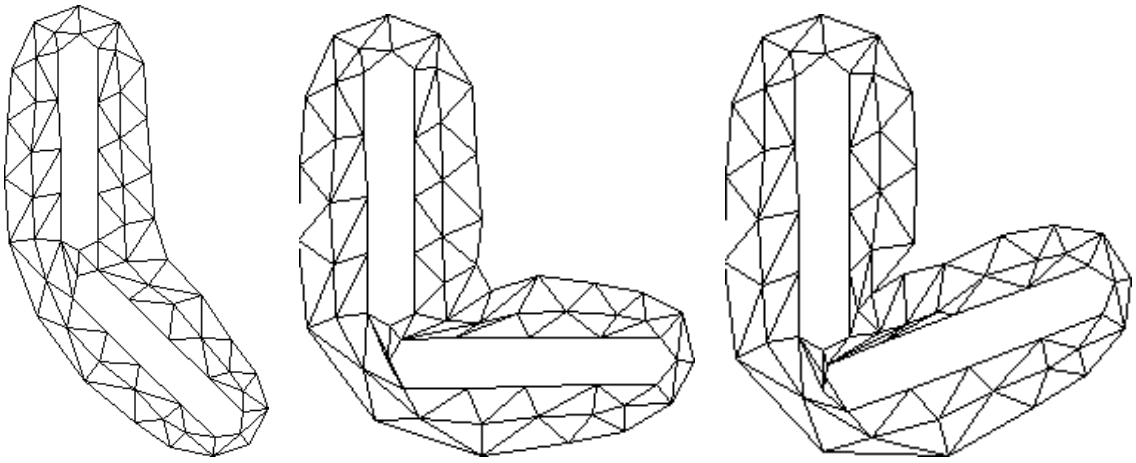

(a) 45 degrees.

(b) 90 degrees.

(c) 110 degrees.

Figure 14: Deformation of new elements at different joint angles.

in figure 13d. As the limb angle is increased further, other elements begin to collapse leading to significant divergence from the "expected" deformation (see figure 13e).
Figure 14 shows the deformation of a mesh composed of the ER-elements under exactly the same conditions. Figure 14a shows the deformation at a joint angle of 45 degrees, and it can be seen that there is significantly less compression compared to the model in 13b. As the joint angle is increased, some elements on the inside of the joint become highly compressed (see fig 14b), but they do not collapse. As well as remaining stable, the model also exhibits effects that occur with real deformable material. For example, slight bulging of the material can be seen and a natural crease appears on the inside of the joint. Finally, figure 14c shows the model at a joint angle of 110 degrees.

6. Conclusion

We have implemented a new element type for MSD models which solves the problem of collapse that occurs in existing models. Images are provided from a simulation (figures 13 and 14) which compare the performance of the new element with a standard element. Although this paper has concentrated on two dimensions, extending the model into three dimensions is straightforward. Rather than using a triangular element, tetrahedral elements are used having damped springs along each of the 6 edges. The edge repulsion now becomes face repulsion in which each of the vertices is repelled by the plane containing the opposite face in the tetrahedron.
Current work is concentrating on implementing the 3D model and we are also considering the development of new force functions which result in more realistic models. We are also interested in modelling other material properties, for example incompressibility, plasticity and fracture[16].

Acknowledgements

This research was funded by the EPSRC.

References

[1] *Siggraph '93 Course Notes: An Introduction to Physically based Modelling*, 1993.

[2] David Baraff and Andrew Witkin. Dynamic simulation of non-penetrating flexible bodies. In Edwin E. Catmull, editor, *Computer Graphics (SIGGRAPH '92 Proceedings)*, volume 26, pages 303–308, July 1992.

[3] John E. Chadwick, David R. Haumann, and Richard E. Parent. Layered construction for deformable animated characters. In Jeffrey Lane, editor, *Computer Graphics (SIGGRAPH '89 Proceedings)*, volume 23, pages 243–252, July 1989.

[4] David T. Chen and David Zeltzer. Pump it up: Computer animation of a biomechanically based model of muscle using the finite element method. In Edwin E. Catmull, editor, *Computer Graphics (SIGGRAPH '92 Proceedings)*, volume 26, pages 89–98, July 1992.

[5] Lee Cooper. Modelling of human skin and tissue for realistic computer animation. Master's thesis, Department of Computer Science, University of Manchester, 1995.

[6] S. Delp, P. Loan, M. Hoy, F. Zajac, S. Fisher, and J. Rosen. An interactive graphics-based model of the lower extremity to study orthopaedic surgical procedures. *IEEE Transactions on Biomedical Engineering*, 37:8, August 1990.

[7] Xiao Qi Deng. *A Finite Element Analysis of Surgery of the Human Facial Tissues.* PhD thesis, Columbia University, 1988.

[8] Marie-Paule Gascuel and Claude Puech. Dynamic Animation of Deformable Bodies. In S. Coquillart, W. Straßer, and P. Stucki, editors, *From Object Modelling to Advance Visual Communication.* Springer–Verlag, 1994.

[9] Jean-Paul Gourret, Nadia Magnenat Thalmann, and Daniel Thalmann. Simulation of object and human skin deformations in a grasping task. In Jeffrey Lane, editor, *Computer Graphics (SIGGRAPH '89 Proceedings)*, volume 23, pages 21–30, July 1989.

[10] Matthew Holton and Simon Alexander. Soft cellular modelling: A technique for the simulation of non-rigid materials. *Computer Graphics: Developments in Virtual Environments (Proceedings of Computer Graphics International '95)*, 1995.

[11] B. Nath. *Fundamentals of finite elements for engineers.* London, Athlone Press, 1974.

[12] Steven Pieper, Joseph Rosen, and David Zeltzer. Interactive graphics for plastic surgery: A task-level analysis and implementation. In David Zeltzer, editor, *Computer Graphics (1992 Symposium on Interactive 3D Graphics)*, volume 25:2, pages 127–134, March 1992.

[13] W.H. Press, B.P. Flannery, Saul A. Teukolsky, and William T. Vetterling. *Numerical Recipes in C.* Cambridge University Press, 1986.

[14] Mark A. Sagar, David Bullivant, Gordon D. Mallinson, Peter J. Hunter, and Ian W. Hunter. A virtual environment and model of the eye for surgical simulation. In Andrew Glassner, editor, *Proceedings of SIGGRAPH '94 (Orlando, Florida, July 24–29, 1994)*, Computer Graphics Proceedings, Annual Conference Series, pages 205–213. ACM SIGGRAPH, ACM Press, July 1994. ISBN 0-89791-667-0.

[15] Demetri Terzopoulos and Kurt Fleischer. Deformable models. *The Visual Computer*, 4(6):306–331, December 1988.

[16] Demetri Terzopoulos and Kurt Fleischer. Modeling inelastic deformation: Viscoelasticity, plasticity, fracture. *Computer Graphics*, 22(4):269–278, August 1988.

[17] Demetri Terzopoulos, John Platt, Alan Barr, and Kurt Fleischer. Elastically deformable models. In Maureen C. Stone, editor, *Computer Graphics (SIGGRAPH '87 Proceedings)*, volume 21, pages 205–214, July 1987.

[18] Shin ya Miyazaki, Masao Ishiguro, Takami Yasuda, Shigeki Yokoi, and Jun ichiro Toriwaki. A study of virtual manipulation of elastic objects. *Computer Graphics: Developments in Virtual Environments (Proceedings of Computer Graphics International '95)*, 1995.